Accounting for super-, plateau- and mesa-rate burning by lead and copper-based ballistic modifiers in double base propellants: a computational study

*Lisette R. Warren,[a] Aaron Rowell,[a] Patrick McMaster,[b] Colin R. Pulham,[a] and Carole A. Morrison[a, *]*

[a] *EaSTCHEM School of Chemistry, University of Edinburgh, The King's Buildings, David Brewster Road, Edinburgh, EH9 3FJ, UK.*

[b] *DOSG-ST1, NH4, MoD Abbey Wood, Bristol, BS34 8JH*

Supplementary Information

S1: Energy rankings and global minimum structures obtained for Pb_xO_y, ($x \leq 6, y \leq x + 3$) clusters from AIRSS/DFT study

S2: Chemical stabilities of Pb_xO_y, ($x \leq 6, y \leq x + 3$) clusters

S3: Energy rankings for sequential carbon attachment to Pb_4O_{4-6}

S4: Radial distribution functions for Pb…Pb distances from carbon binding study to Pb_4O_{4-6}

S5: Fitting functions for lines of best fit for the local force constants vs bond length plots

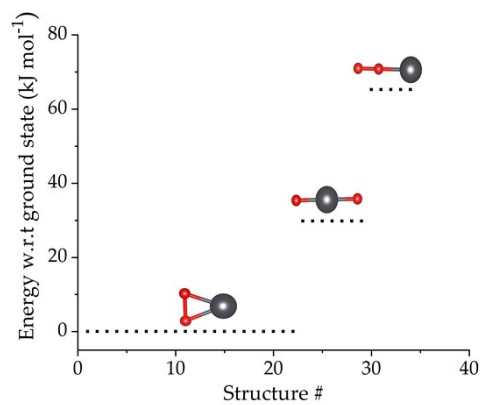**S6:** Energy rankings for sequential carbon attachment to Cu_5O_5

S7: Radial distribution functions for Cu…Cu distances from carbon binding study to Cu_5O_5

S8: Small molecule binding study to metal oxide clusters: NO_2 and CH_2O bond weakening effects
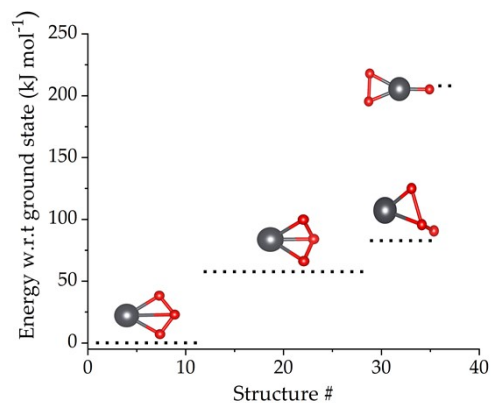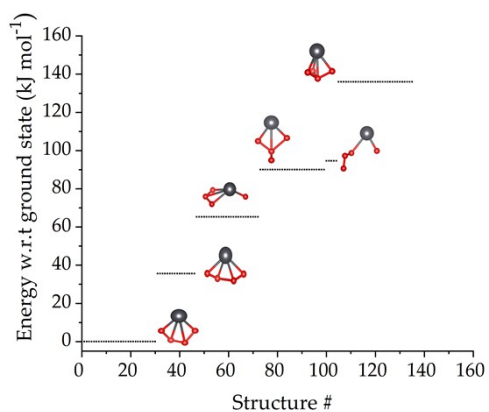
S9: Individual binding modes for NO_2 and CH_2O to $Pb_4O_{4-6}C_{0-12}$ and $Cu_5O_5C_{0-12}$ clusters

S10: Exploring the effects of varying electronic spin states for cluster series $Pb_4O_{4-6}C_{3,12}$ and $Cu_5O_5C_{3,12}$

S1: Energy rankings and global minimum structures obtained for Pb_xO_y, $(x \le 6, y \le x + 3)$ clusters from AIRSS/DFT study
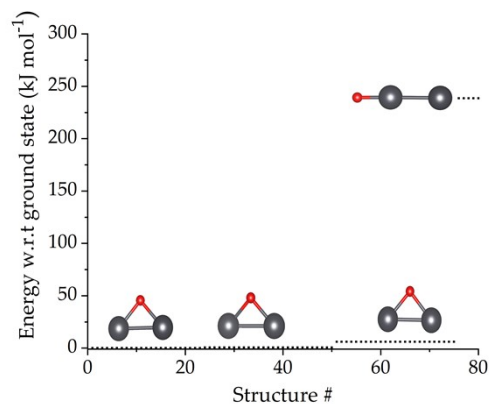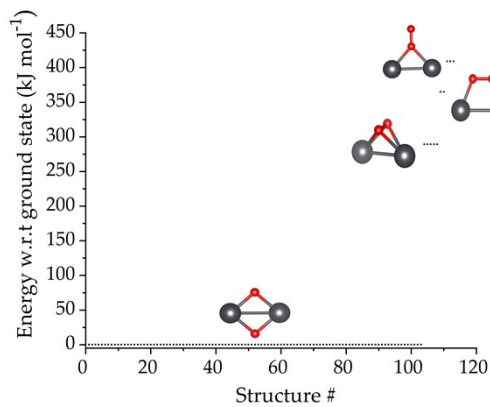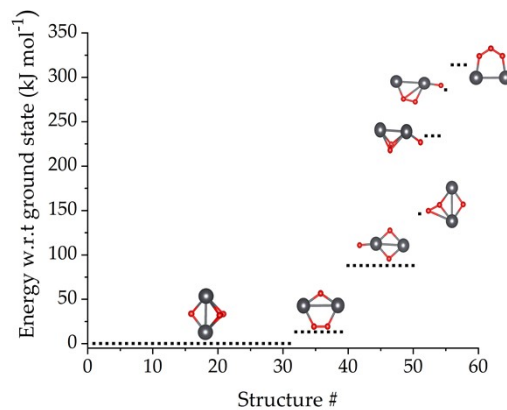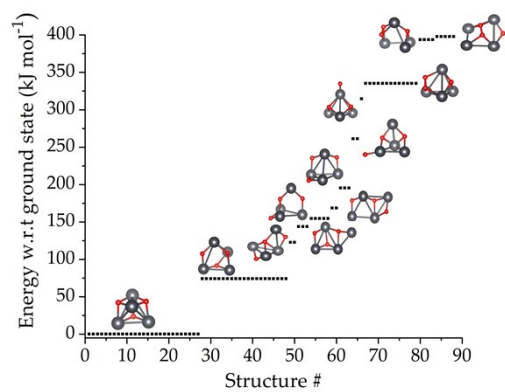

PbO$_2$

PbO$_3$

PbO$_4$

Pb$_2$O

Pb$_2$O$_2$

Pb$_2$O$_3$

Pb$_2$O$_4$

Pb$_2$O$_5$

Pb$_3$O$_2$

Pb$_3$O$_3$

Pb$_3$O$_4$

Pb$_3$O$_5$

Pb$_3$O$_6$

Pb$_4$O$_3$
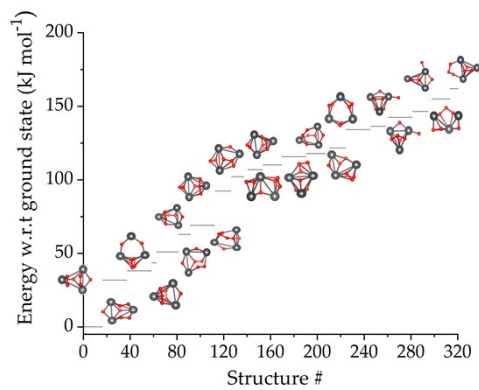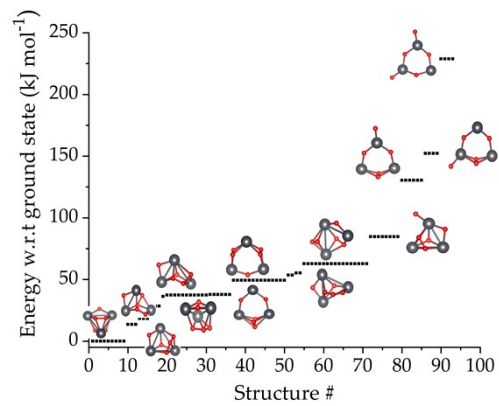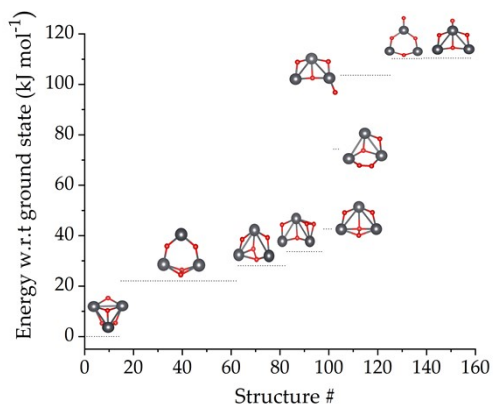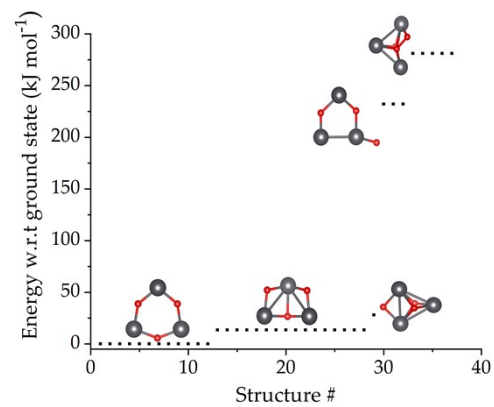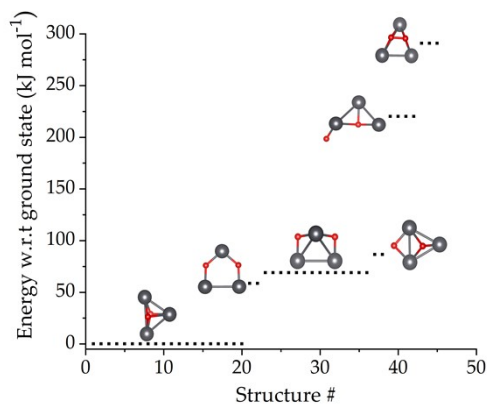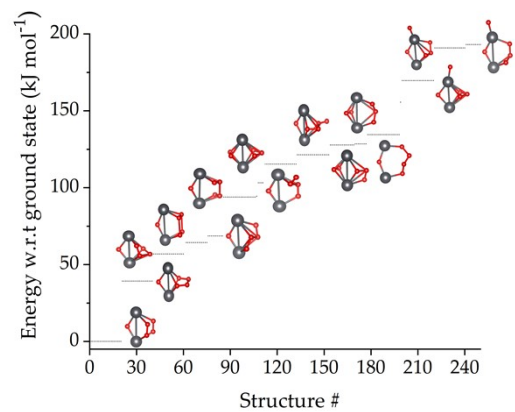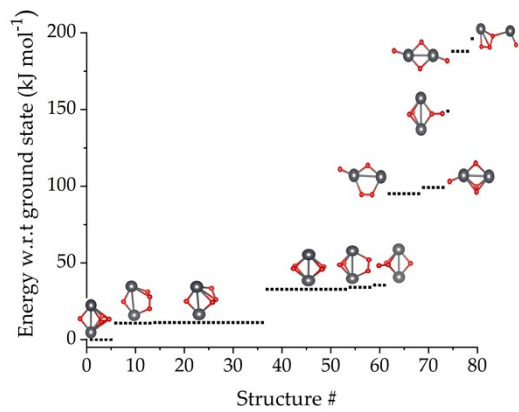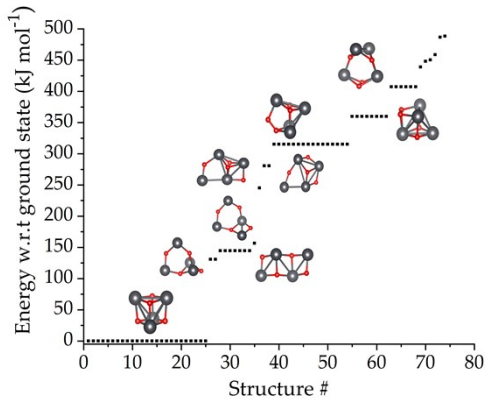
Pb$_4$O$_4$
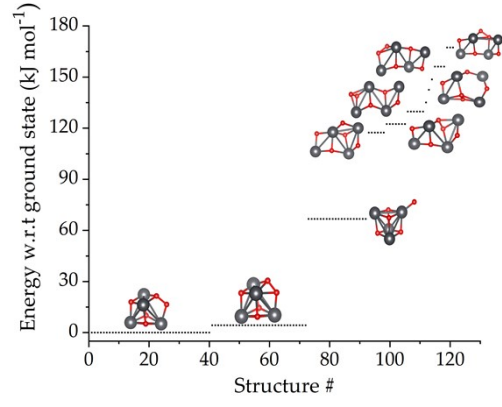
Pb$_4$O$_5$
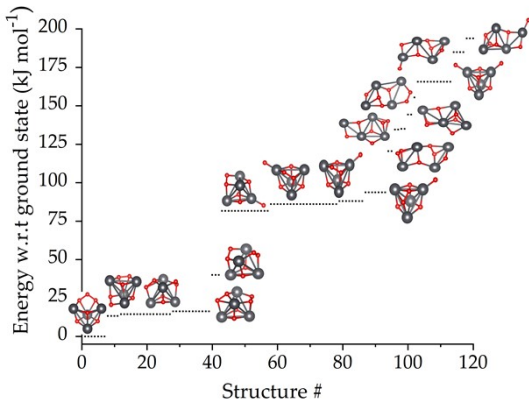
Pb$_4$O$_6$
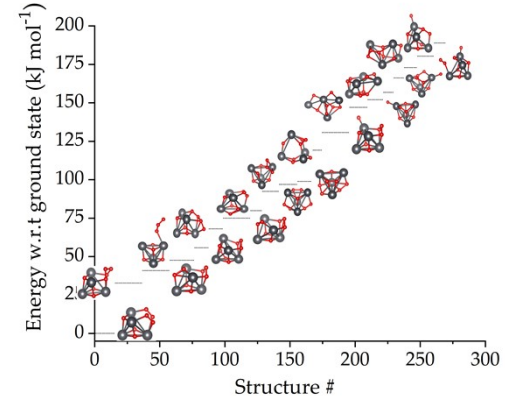
Pb$_4$O$_7$

Pb$_5$O$_4$

Pb$_5$O$_5$

Pb$_5$O$_6$

Pb$_5$O$_7$

Pb$_5$O$_8$

Pb$_6$O$_5$

Pb$_6$O$_6$

Pb$_6$O$_7$

Pb$_6$O$_8$

Pb$_6$O$_9$
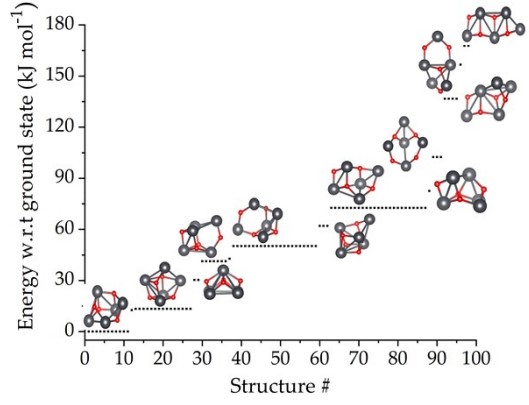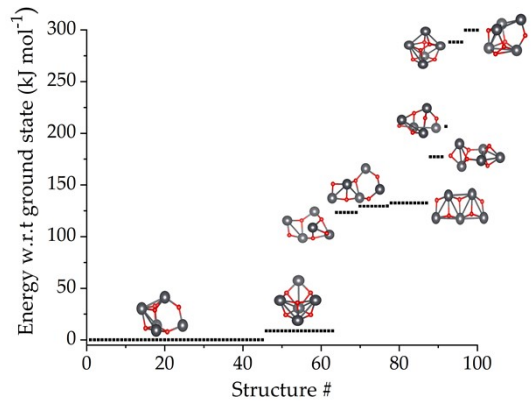
Figure S1 Possible structures of small clusters of Pb$_x$O$_y$ and their respective multiplicities generated by *ab initio* random structure searching.

The lowest energy structures thus obtained are summarised in Figure S2. The main structural features observed for the lead oxi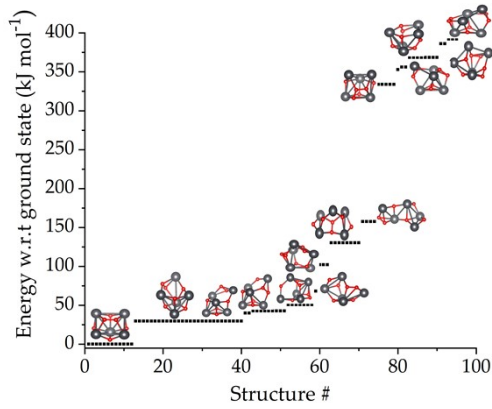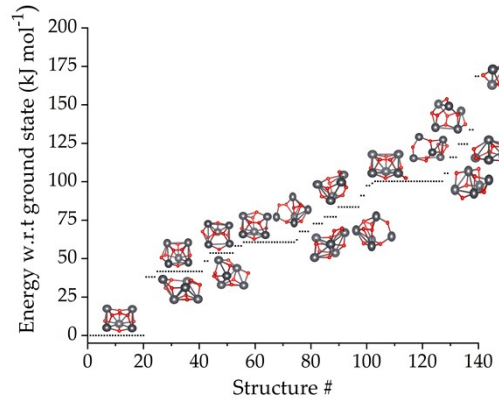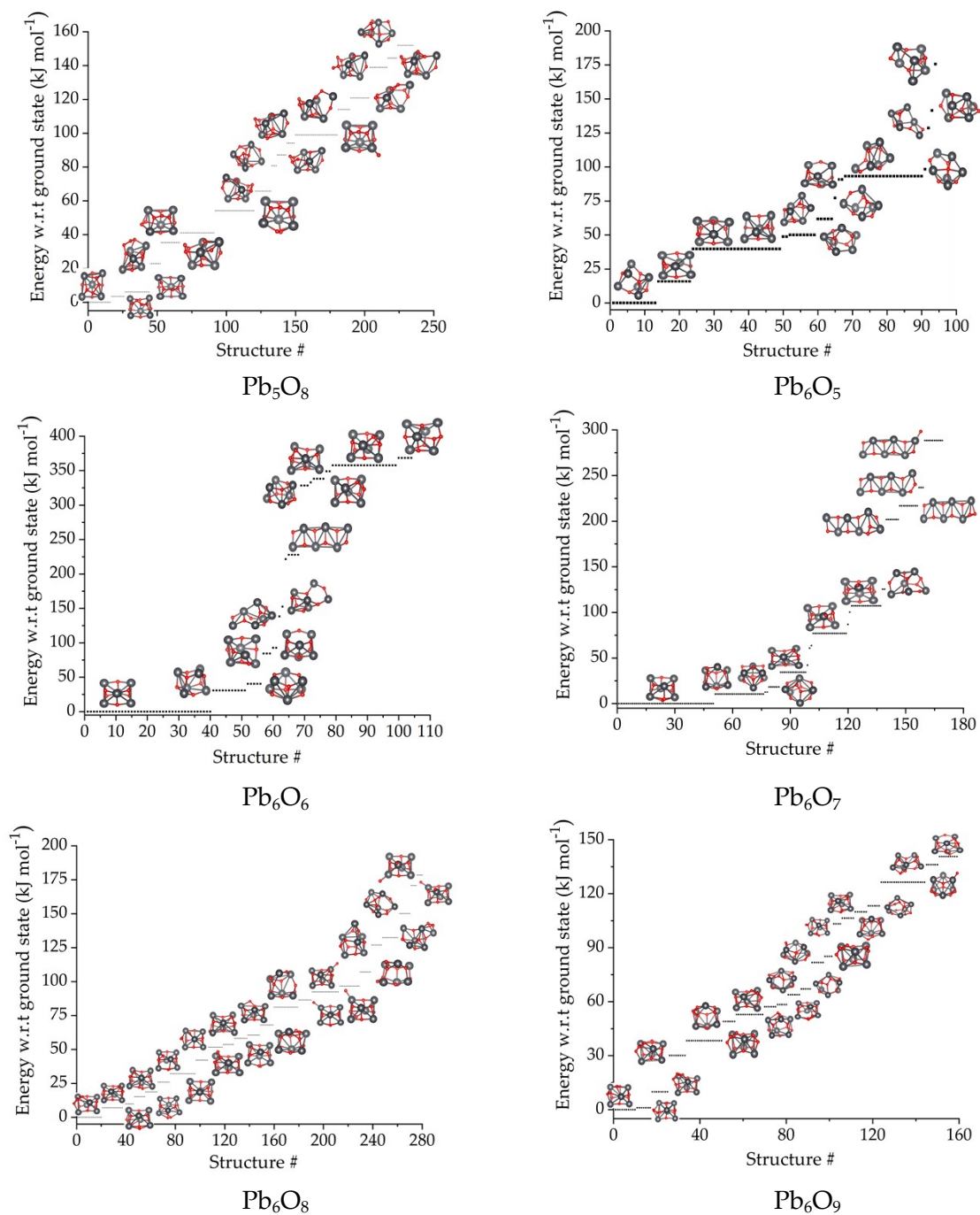de clusters are that Pb_xO_y ($x = y$) appears to result in highly symmetric clusters, in agreement with experimental data.[1-4] The geometries for the O-rich ($x < y$) and Pb-rich ($x > y$) can be viewed as small variants of their nearest $(PbO)_x$ global minimum structure. Many of the clusters are based on oxygen or lead insertion into a Pb_2O_2 ring or Pb_4O_4 cube. In low-oxygen environments, oxygen atoms generally form μ_2-bridging sites (when $x \leq 3$) or μ_3-bridging sites (when $x \geq 4$) until high symmetry structures are generated for equal Pb/O ratios. The oxygen-rich clusters all feature oxygen atoms binding together.
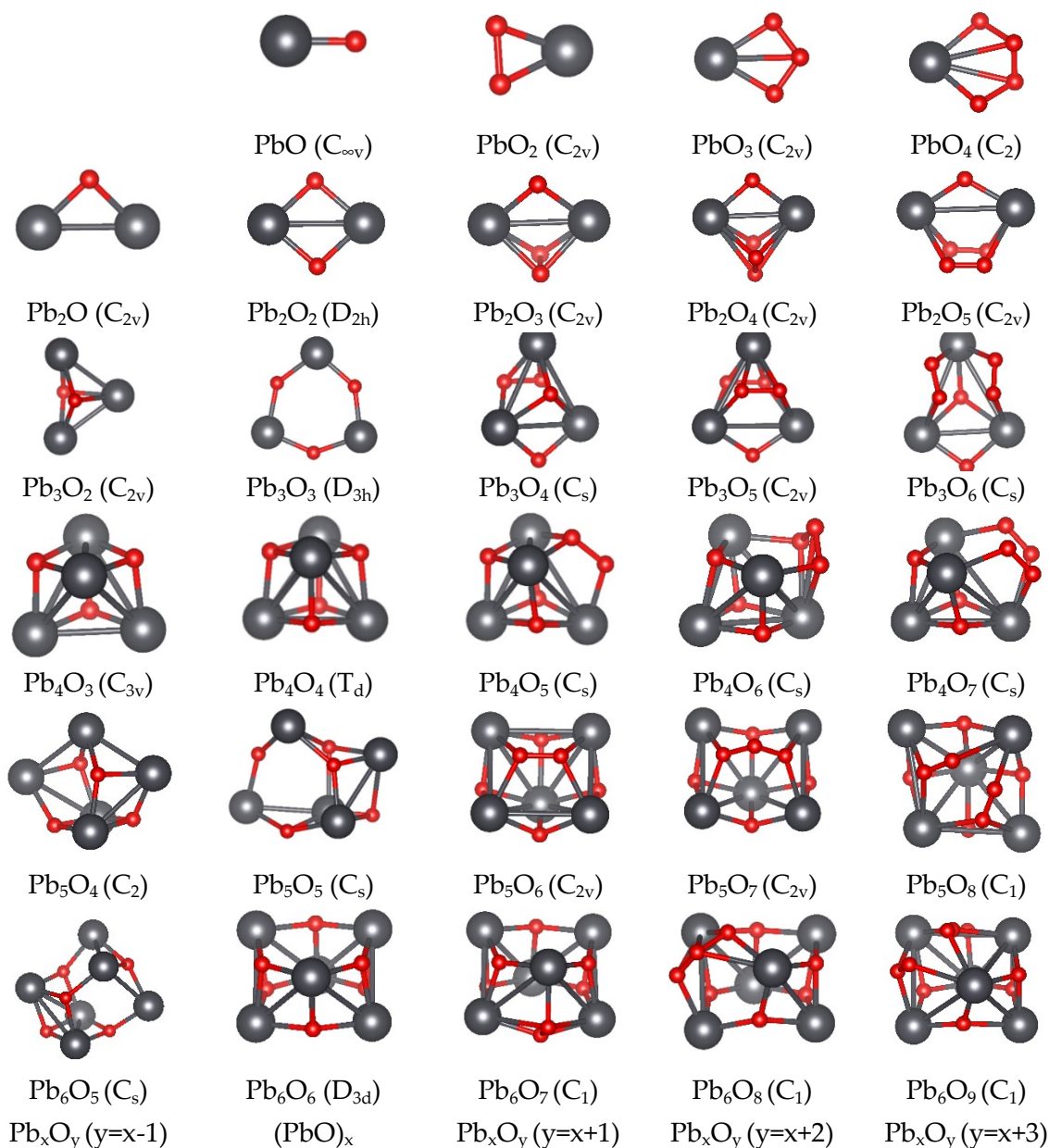

| | PbO ($C_{\infty v}$) | PbO$_2$ (C_{2v}) | PbO$_3$ (C_{2v}) | PbO$_4$ (C_2) |

| Pb$_2$O (C_{2v}) | Pb$_2$O$_2$ (D_{2h}) | Pb$_2$O$_3$ (C_{2v}) | Pb$_2$O$_4$ (C_{2v}) | Pb$_2$O$_5$ (C_{2v}) |

| Pb$_3$O$_2$ (C_{2v}) | Pb$_3$O$_3$ (D_{3h}) | Pb$_3$O$_4$ (C_s) | Pb$_3$O$_5$ (C_{2v}) | Pb$_3$O$_6$ (C_s) |

| Pb$_4$O$_3$ (C_{3v}) | Pb$_4$O$_4$ (T_d) | Pb$_4$O$_5$ (C_s) | Pb$_4$O$_6$ (C_s) | Pb$_4$O$_7$ (C_s) |

| Pb$_5$O$_4$ (C_2) | Pb$_5$O$_5$ (C_s) | Pb$_5$O$_6$ (C_{2v}) | Pb$_5$O$_7$ (C_{2v}) | Pb$_5$O$_8$ (C_1) |

| Pb$_6$O$_5$ (C_s) | Pb$_6$O$_6$ (D_{3d}) | Pb$_6$O$_7$ (C_1) | Pb$_6$O$_8$ (C_1) | Pb$_6$O$_9$ (C_1) |
| Pb$_x$O$_y$ (y=x-1) | (PbO)$_x$ | Pb$_x$O$_y$ (y=x+1) | Pb$_x$O$_y$ (y=x+2) | Pb$_x$O$_y$ (y=x+3) |

Figure S2. Global minimum energy structures of Pb$_x$O$_y$ series found by AIRSS. Legend: dark grey (Pb) and red (O). Point group symmetry shown in brackets.
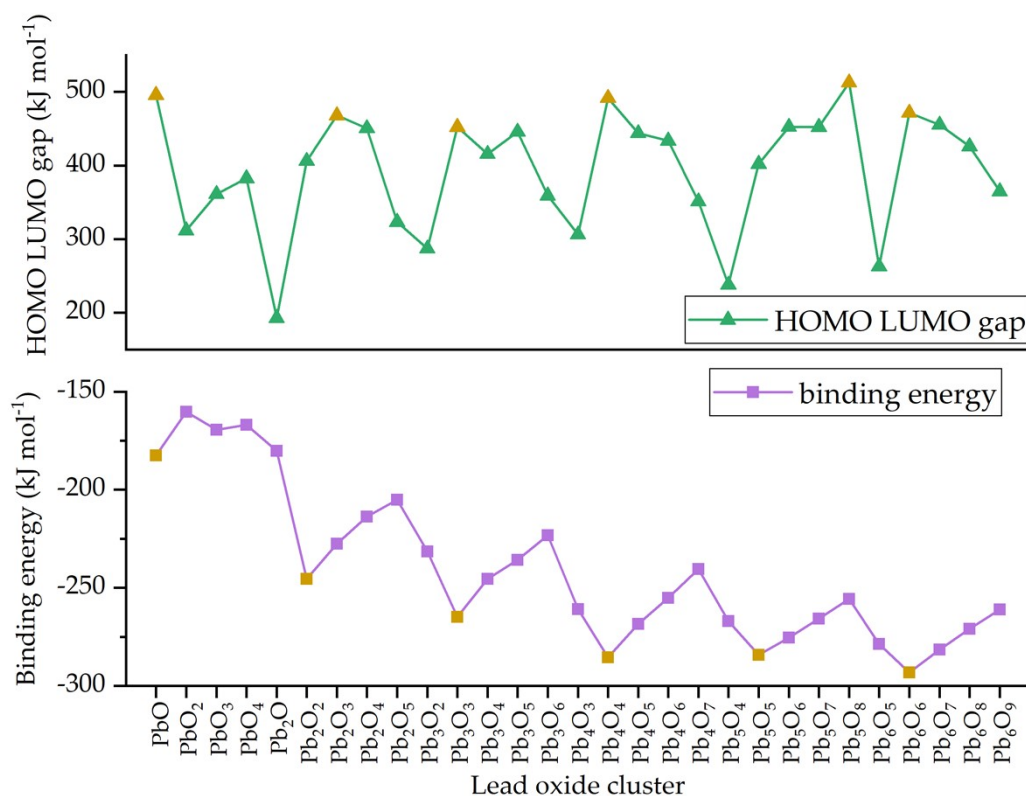
Figure S3. HOMO LUMO gaps (top) and average binding energies of Pb$_x$O$_y$ clusters (bottom). Gold data points denote most negative binding energy and largest HOMO-LUMO gap for each Pb$_x$ series. Binding energies and HOMO-LUMO gaps computed with the SDD/def2TZV basis set and PBE0-D3BJ level of theory using Gaussian16.

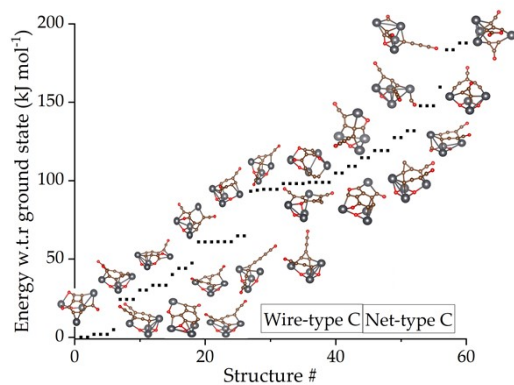## S3: Energy rankings for sequential carbon attachment to Pb_4O_{4-6}

Energy rankings for sequential carbon additions (3-12 atoms) to Pb_4O_{4-6}, shown up to 200 kJ mol^{-1} above the lowest energy structure for C_3 to C_9 and 250 kJ mol^{-1} for C_{12}.
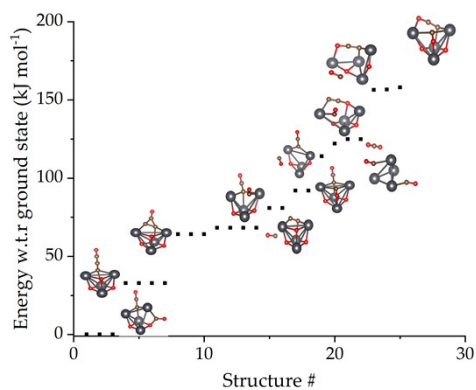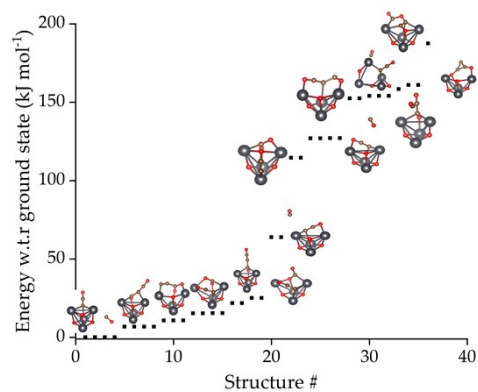

$Pb_4O_4C_3$
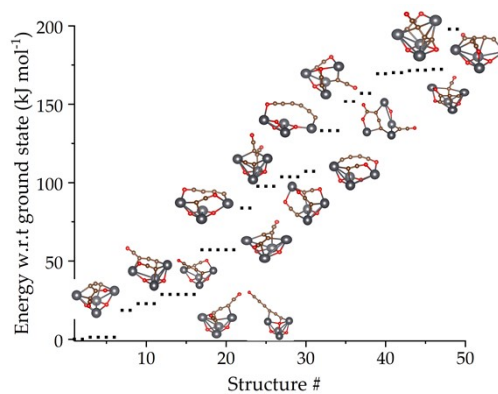
$Pb_4O_4C_6$

$Pb_4O_4C_9$
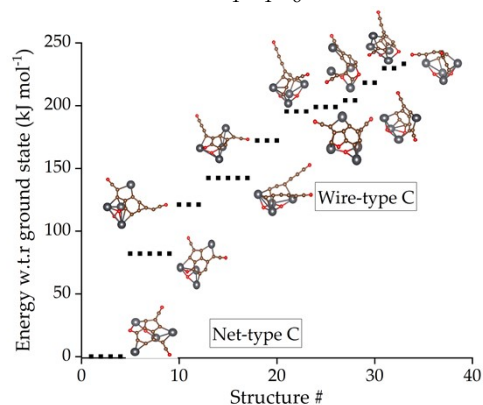
$Pb_4O_4C_{12}$

$Pb_4O_5C_3$
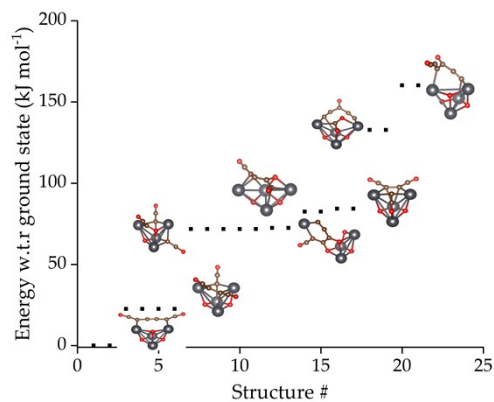
$Pb_4O_5C_6$
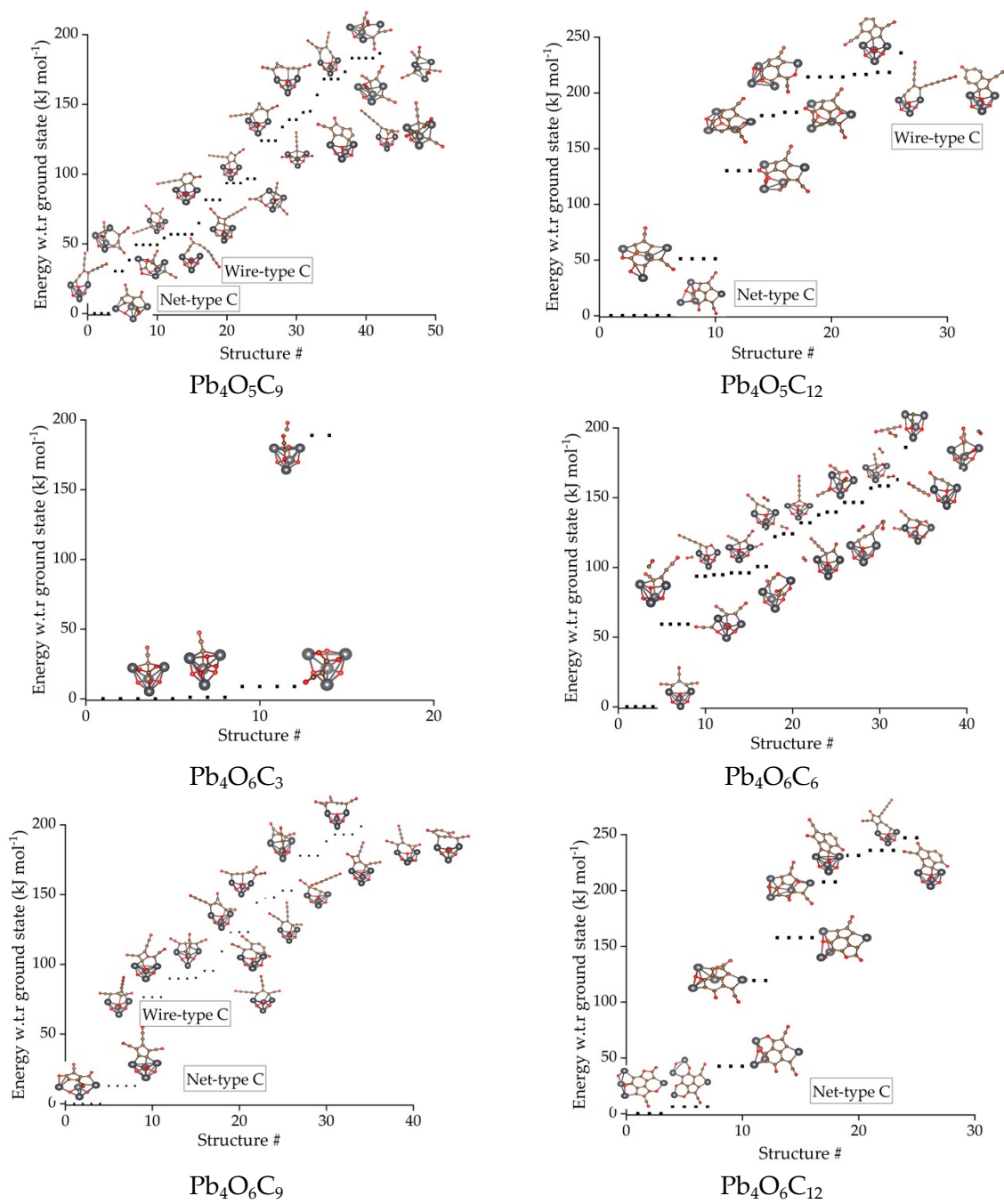
Figure S4 Possible structures for carbon addition to Pb_4O_{4-6} generated by *ab initio* random structure searching.

S4: Radial distribution functions for Pb…Pb distances from carbon binding study to Pb$_4$O$_{4-6}$
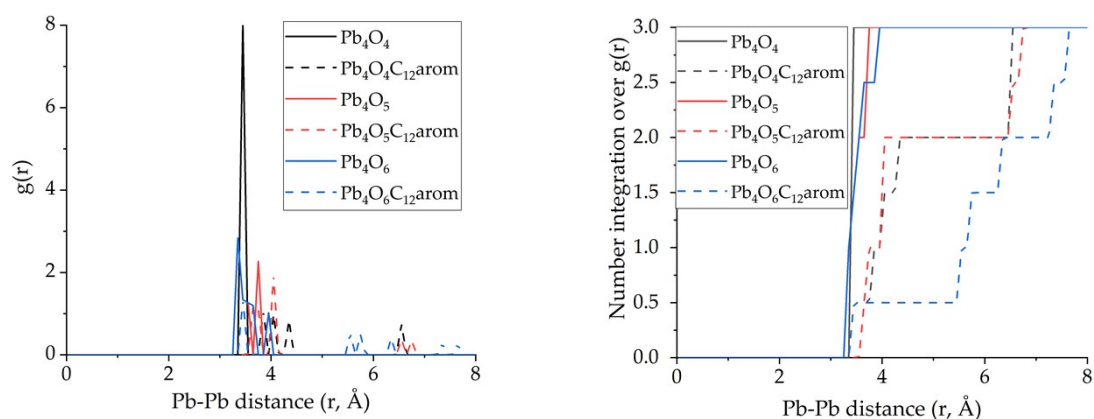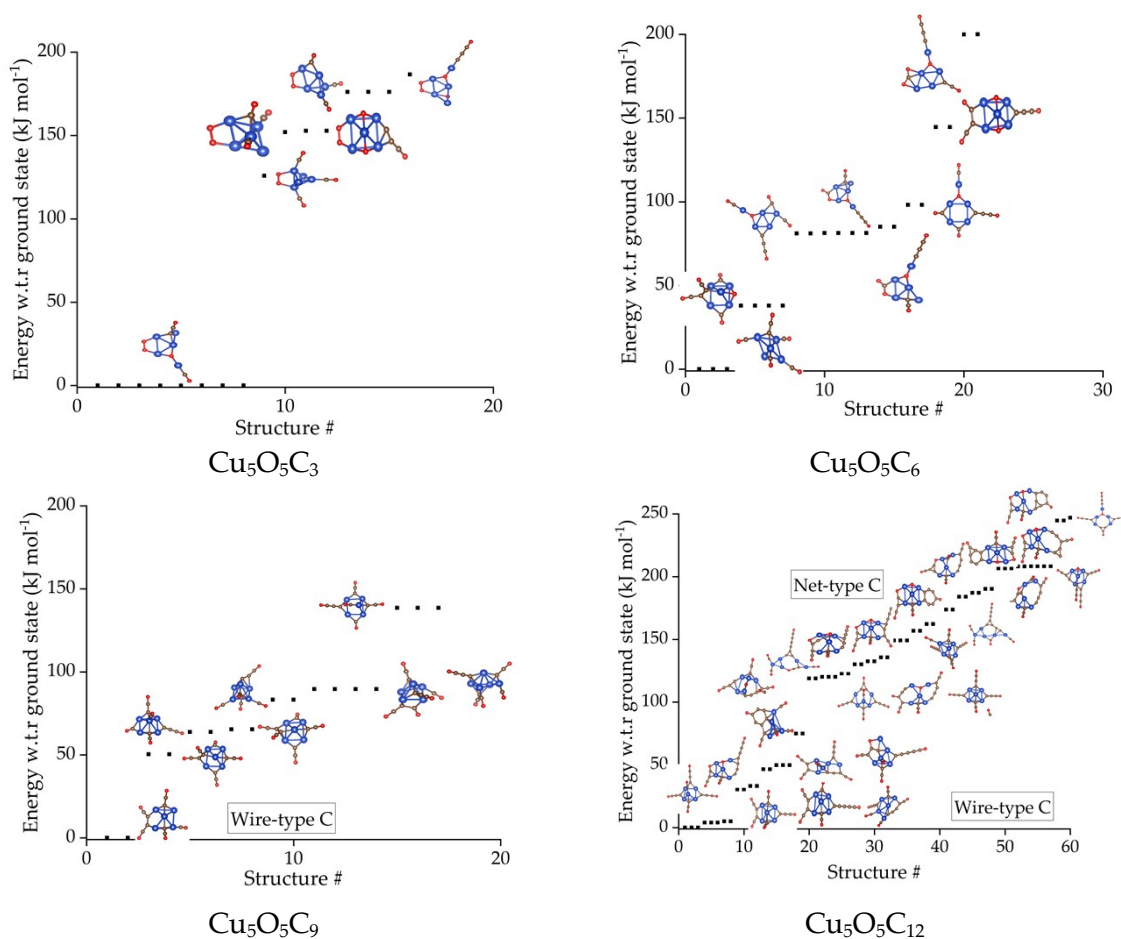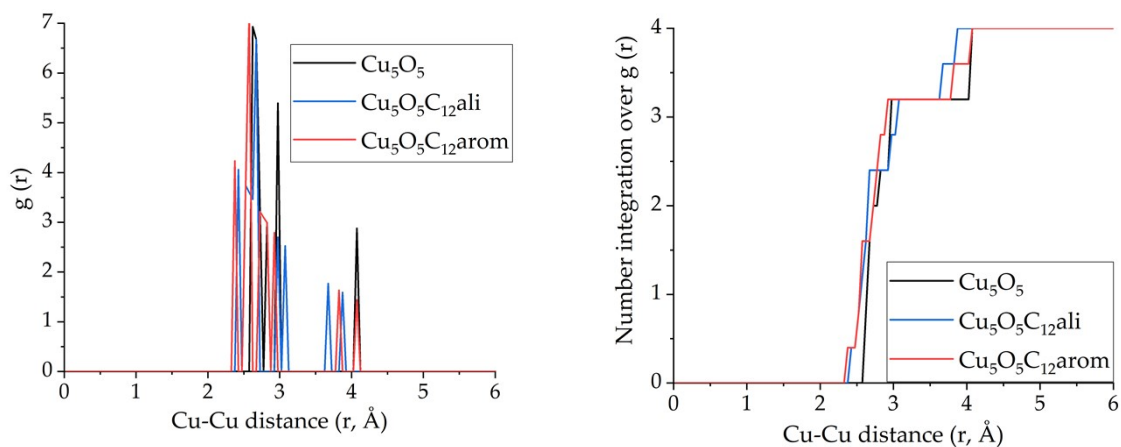

Figure S5. Radial distribution function g(r) (left) and integration over g(r) (right) for Pb-Pb distances within Pb$_4$O$_{4-6}$, and aromatic-C bound clusters.

S5: Fitting functions for lines of best fit for the local force constants vs bond length plots

Table S1. Fitting functions for line of best fits for M$_x$O$_y$C$_{12}$ for lead and copper oxide clusters.

Chemical bond	Figure	Line of best fit	R^2
Pb-C	7, 9b	$y = 768e^{(-\frac{x}{0.3907})} - 0.7873$	0.945
Pb-O (carbon-bound lead oxide)	7	$y = 8267e^{(-\frac{x}{0.2498})} + 0.0079$	0.963
C-C (carbon-bound lead oxide)	7	$y = 9271e^{(-\frac{x}{0.1888})} + 0.7497$	0.955
C-O (carbon-bound lead oxide)	7	$y = 26647e^{(-\frac{x}{0.1575})} + 0.4292$	0.996
Cu-C	9	$y = 693e^{(-\frac{x}{0.1957})} - 0.9271$	0.853
Cu-O (carbon-bound copper oxide)	9a	$y = 400e^{(-\frac{x}{0.4129})} - 2.380$	0.967

C-C (carbon-bound copper oxide)	9a	$y = 29981e^{\left(-\frac{x}{0.1612}\right)} + 0.5073$	0.933
C-O (carbon-bound copper oxide)	9a	$y = 7532e^{\left(-\frac{x}{0.1957}\right)} - 3.077$	0.912

S6: Energy rankings for sequential carbon attachment to Cu_5O_5

Energy rankings for sequential carbon additions (3-12 atoms) to Cu_5O_5, shown up to 500 kJ mol^{-1} above lowest energy structure.

$Cu_5O_5C_3$

$Cu_5O_5C_6$

$Cu_5O_5C_9$

$Cu_5O_5C_{12}$

Figure S5. Possible structures for carbon addition to Cu_5O_5 generated by *ab initio* random structure searching.

S7: Radial distribution function for Cu…Cu distances from carbon binding study to Cu$_5$O$_5$

Figure S6. Radial distribution function g(r) (left) and integration over g(r) (right) for Cu...Cu distances within Cu$_5$O$_5$, and aliphatic-C and aromatic-C bound clusters.

S8: Small molecule binding study to metal oxide clusters: NO$_2$ and CH$_2$O bond weakening effects

Looking next to the activation of N–O and C–O through bond weakening, graphs of local force constants vs bond length are reported in Figure S7, with the trend line obtained from Christopher et al[5] (black line) which originates from the N–O and C–O bond strengths from a larger data set of energetic molecules. The strength of the C–O and N–O bonds in CH$_2$O and NO$_2$ are strong (black square), at ca. 12 and 9 mDyn Å^{-1} respectively.

For lead oxide clusters, binding of the small molecules to any cluster results in significant bond weakening, to ca. 4 mDyn Å^{-1}; ~ 60 % reduction in the strength of the bonds. Thus it can be concluded that all species are acting as Lewis acids, and catalytically activate both N–O and C–O bonds.

For copper oxide clusters, the effect for CH$_2$O binding is similar in the presence of carbon (where binding largely occurs through carbon atoms), whilst binding to copper oxide clusters results in less bond weakening, ca. 50 %. For NO$_2$ binding, the bond weakening effect is also less pronounced for bare copper oxide. The introduction of carbon provides carbon sites for NO$_2$ binding, acting as Lewis acids.
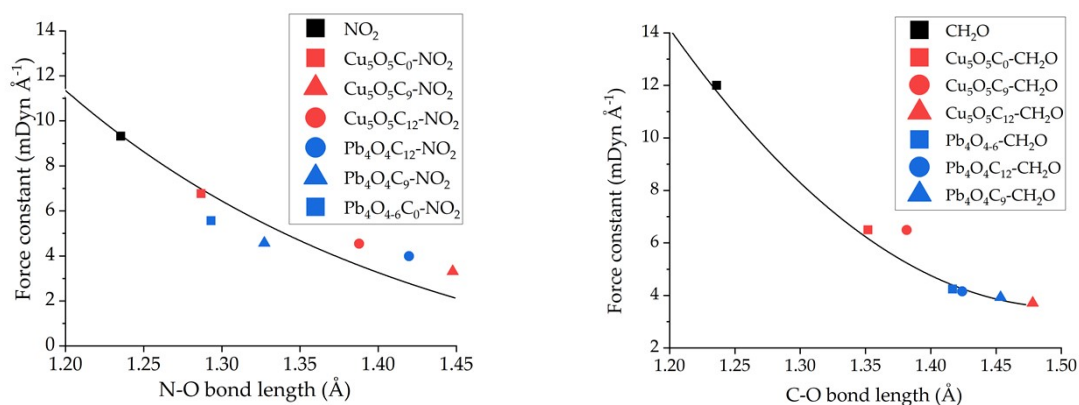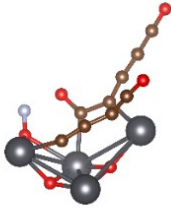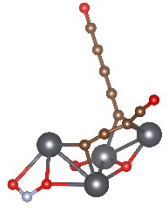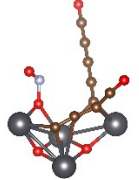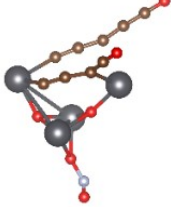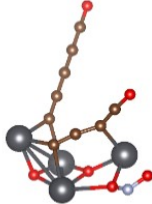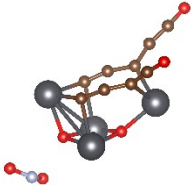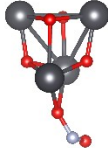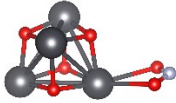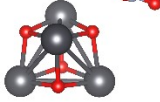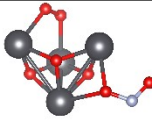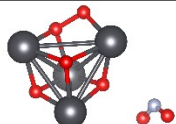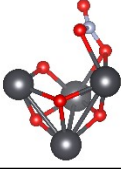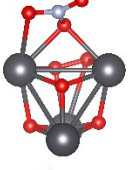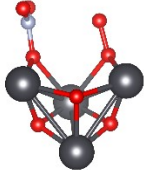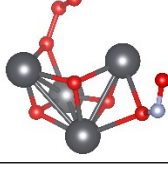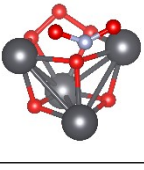
Figure S7. N-O (left) and C-O (right) bond weakening from NO_2 and CH_2O binding to lead and copper oxide clusters with varying carbon content for Pb_4O_4 and Cu_5O_5. Trend line from ref 5.

S9: Individual binding modes for NO_2 and CH_2O to $Pb_4O_{4-6}C_{0-12}$ and $Cu_5O_5C_{0-12}$ clusters
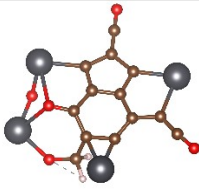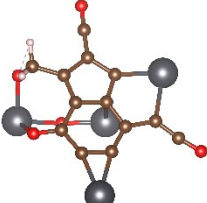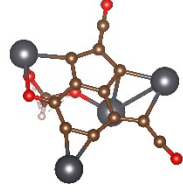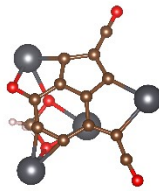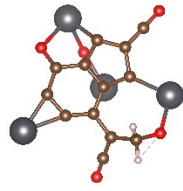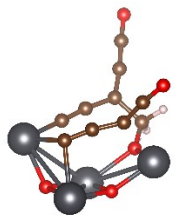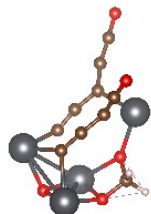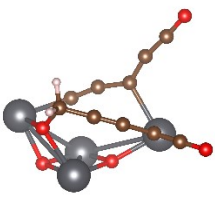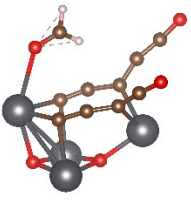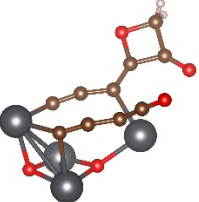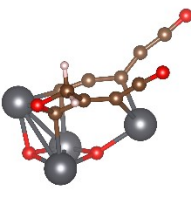
Table S2. NO_2 binding to Pb_4O_{4-6} and $Pb_4O_4C_{9,12}$

System [Spin]	Binding energy (kJ mol^{-1})	Optimised geometry	Binding energy (kJ mol^{-1})	Optimised geometry
$Pb_4O_4C_{12}$ (aromatic) [Doublet]	-274*		-168	
	-267		-151	
	-249		-140	
	-232*		-85*	

Pb$_4$O$_4$C$_9$ (aliphatic) [Doublet]	-132*		-113	
	-129		-79	
	-129		16	
Pb$_4$O$_4$ [Doublet]	1		30	
	13			
Pb$_4$O$_5$ [Doublet]	-48		14	
	-39			
Pb$_4$O$_6$ [Doublet]	-80		-2	
	-35		15	

*Binding mode breaks N–O bond.

Table S3. CH_2O binding to Pb_4O_{4-6} and $Pb_4O_4C_{9,12}$.

System [Spin]	Binding energy (kJ mol^{-1})	Optimised geometry	Binding energy (kJ mol^{-1})	Optimised geometry
$Pb_4O_4C_{12}$ (aromatic) [Singlet]	-232		-61	
	-158		-39	
	-74		-36	
$Pb_4O_4C_9$ (aliphatic) [Singlet]	-154		-58	
	-116		-1	
	-101		8	
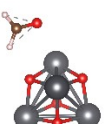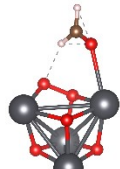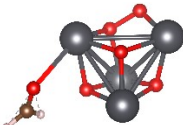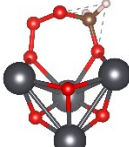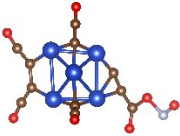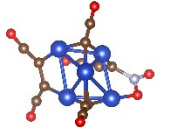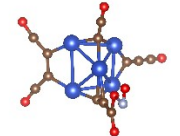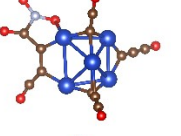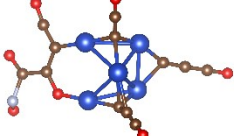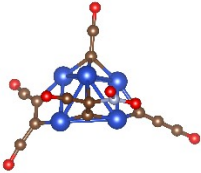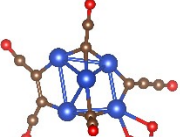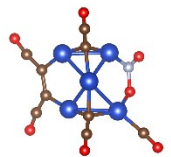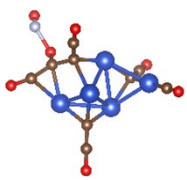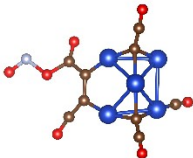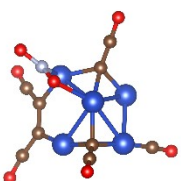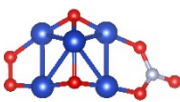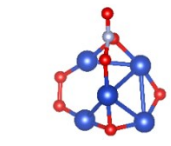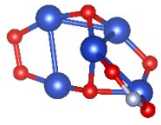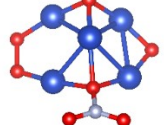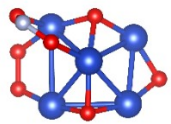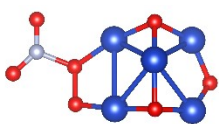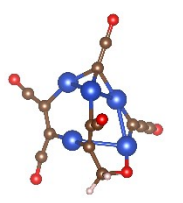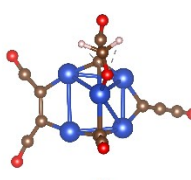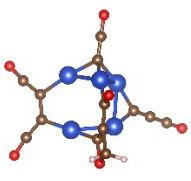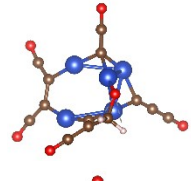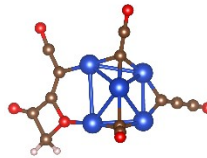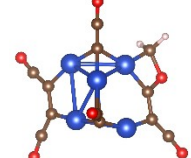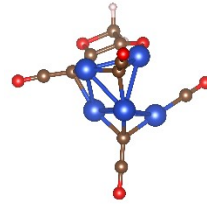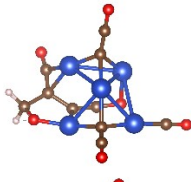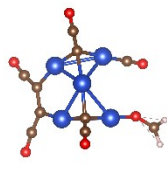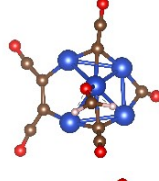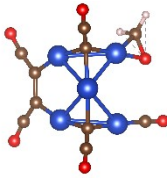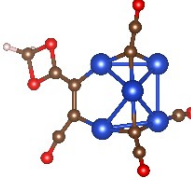
Pb_4O_4 [Singlet]	-63		13
	-62		
Pb_4O_5 [Singlet]	-59		2.5
	-45		11
Pb_4O_6 [Singlet]	-68		9
	-34		

Table S4. NO_2 binding to Cu_5O_5 and $Cu_5O_5C_{9,12}$.

System [Spin]	Binding energy (kJ mol^{-1})	Optimised geometry	Binding energy (kJ mol^{-1})	Optimised geometry
$Cu_5O_5C_{12}$ (aliphatic) [Triplet]	-137		-70	
	-132		-9	
	-130*		2	
	-86			
$Cu_5O_5C_9$ (aliphatic) [Singlet]	-133		-32	
	-50		3	
Cu_5O_5 [Triplet]	-139		-40	
	-83		9	
	-52		22	

*Binding mode breaks N–O bond.

Table S5. CH_2O binding to Cu_5O_5 and $Cu_5O_5C_{9,12}$.

System [Spin]	Binding energy (kJ mol^{-1})	Optimised geometry	Binding energy (kJ mol^{-1})	Optimised geometry
$Cu_5O_5C_{12}$ (aliphatic) [Quartet]	-64		-16	
	-32		24	
	-30		41	
$Cu_5O_5C_9$ (aliphatic) [Doublet]	-142		-35	
	-74		4	
	-55		97	
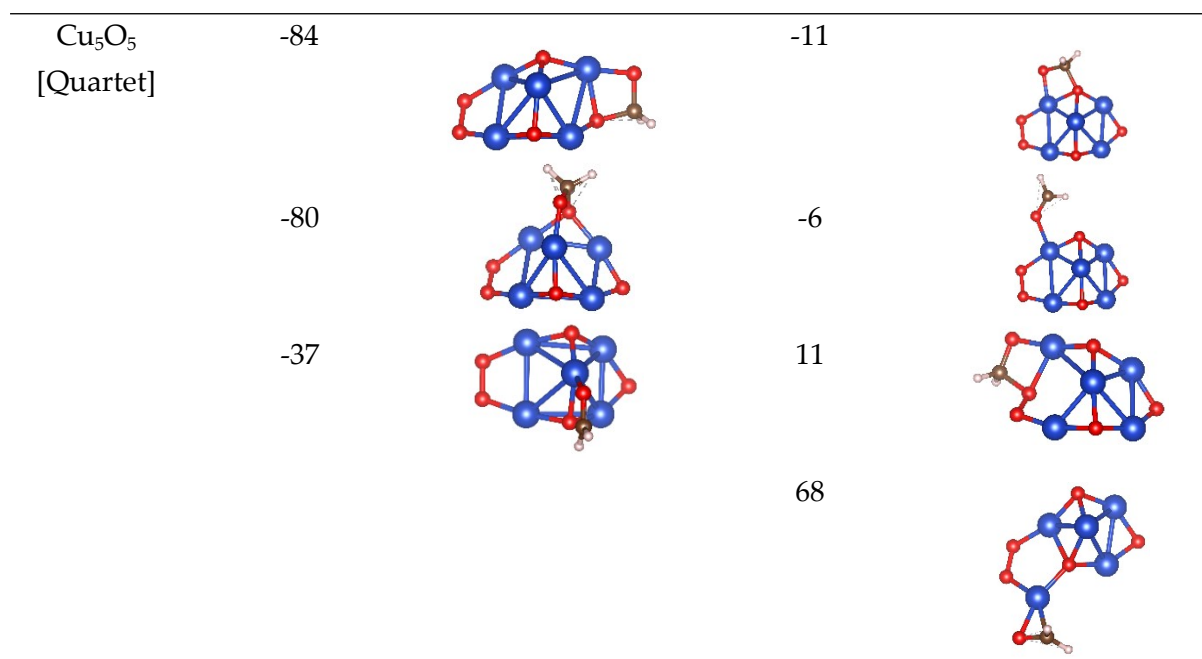
Cu₅O₅ [Quartet]	-84		-11	
	-80		-6	
	-37		11	
			68	

S10: Exploring the effects of varying electronic spin states for cluster series Pb₄O₄₋₆C₃,₁₂ and Cu₅O₅C₃,₁₂

Table S6. Energies for the lowest energy structure vs. spin state for sequential addition of carbon to Pb_4O_{4-6} and Cu_5O_5. Energy differences compared to the most stable spin states are given in kJ mol^{-1}. Most stable spin states are highlighted in bold.
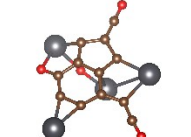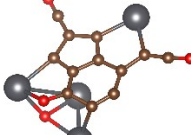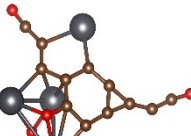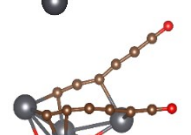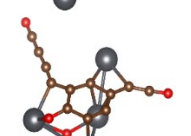
System							
$Pb_4O_4C_3$	Spin	**1**	3	5	7	9	11
	Energy (A.U.)	**-428.66**	-428.62	-428.58	-428.50	-428.40	-428.31
	Energy difference (kJ mol^{-1})	**0**	+90	+199	+419	+660	+899
$Pb_4O_4C_6$	Spin	**1**	3	5	7	9	11
	Energy (A.U.)	**-542.75**	-542.67	-542.60	-542.51	-542.42	-542.30
	Energy difference (kJ mol^{-1})	**0**	+203	+389	+626	+850	+1184
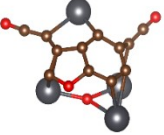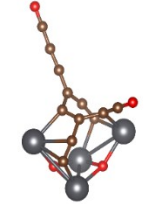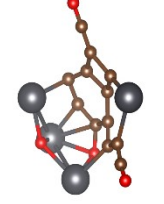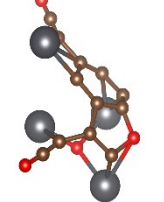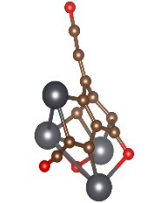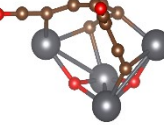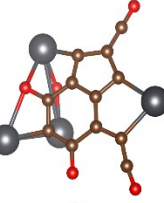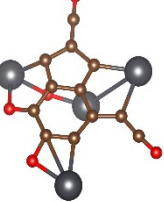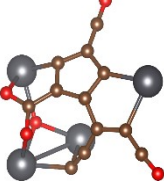
$Pb_4O_4C_9$	Spin	**1**	3	5	7	9	11
	Energy (A.U.)	**-656.78**	-656.77	-656.69	-656.62	-656.52	-656.40
	Energy difference (kJ mol^{-1})	**0**	+23	+222	+407	+687	+1000
$Pb_4O_4C_{12}$	Spin	**1**	3	5	7	9	11
	Energy (A.U.)	**-770.91**	-770.88	-770.85	-770.79	-770.74	-770.64
	Energy difference (kJ mol^{-1})	**0**	+82	+166	+327	+460	+734
$Pb_4O_5C_3$	Spin	**1**	3	5	7	9	11
	Energy (A.U.)	**-503.84**	-503.75	-503.64	-503.56	-503.45	-503.34
	Energy difference (kJ mol^{-1})	**0**	+230	+518	+737	+1002	+1308
$Pb_4O_5C_6$	Spin	**1**	3	5	7	9	11
	Energy (A.U.)	**-617.91**	-617.86	-617.76	-617.68	-617.60	-617.51
	Energy difference (kJ mol^{-1})	**0**	+137	+394	+603	+822	+1043
$Pb_4O_5C_9$	Spin	**1**	3	5	7	9	11
	Energy (A.U.)	**-731.95**	-731.89	-731.83	-731.74	-731.62	-731.55
	Energy difference (kJ mol^{-1})	**0**	+171	+310	+541	+864	+1049
$Pb_4O_5C_{12}$	Spin	1	**3**	5	7	9	11
	Energy (A.U.)	-846.09	**-846.11**	-846.05	-845.98	-845.92	-845.83
	Energy difference (kJ mol^{-1})	+48	**0**	+160	+326	+484	+723
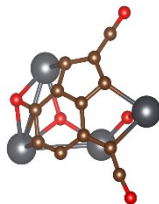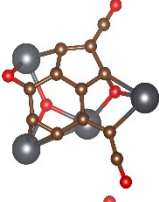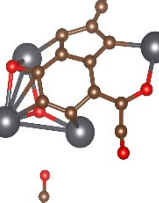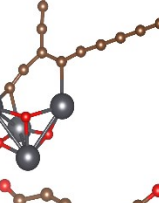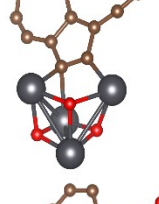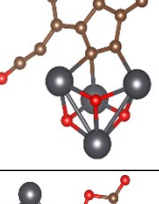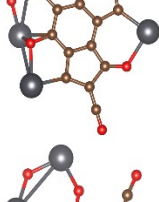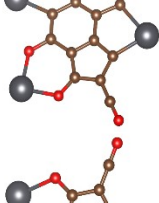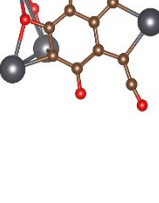
$Pb_4O_6C_3$	Spin	**1**	3	5	7	9	11
	Energy (A.U.)	**-579.04**	-578.95	-578.88	-578.77	-578.66	-578.52
	Energy difference (kJ mol⁻¹)	**0**	+251	+438	+732	+1000	+1383
$Pb_4O_6C_6$	Spin	**1**	3	5	7	9	11
	Energy (A.U.)	**-693.07**	-693.05	-692.94	-692.86	-692.76	-692.67
	Energy difference (kJ mol⁻¹)	**0**	+71	+337	+563	+818	+1052
$Pb_4O_6C_9$	Spin	**1**	3	5	7	9	11
	Energy (A.U.)	**-807.18**	-807.15	-807.09	-807.03	-806.94	-806.84
	Energy difference (kJ mol⁻¹)	**0**	+71	+232	+393	+626	+874
$Pb_4O_6C_{12}$	Spin	**1**	3	5	7	9	11
	Energy (A.U.)	**-921.33**	-921.31	-921.25	-921.15	-921.07	-920.95
	Energy difference (kJ mol⁻¹)	**0**	+39	+212	+451	+671	+997
$Cu_5O_5C_3$	Spin	**2**	4	6	8	10	
	Energy (A.U.)	**-1476.34**	-1476.30	-1476.20	-1476.09	-1476.01	
	Energy difference (kJ mol⁻¹)	**0**	+107	+368	+652	+864	
$Cu_5O_5C_6$	Spin	**2**	4	6	8	10	
	Energy (A.U.)	**-1590.50**	-1590.47	-1590.41	-1590.30	-1590.14	
	Energy difference (kJ mol⁻¹)	**0**	+94	+246	+532	+961	
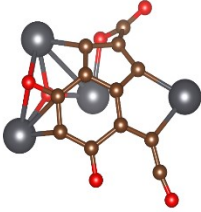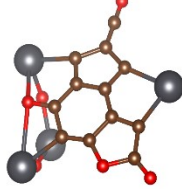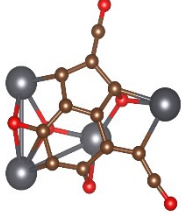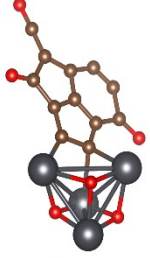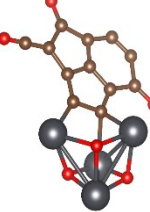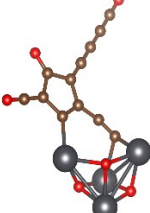
Cu$_5$O$_5$C$_9$	Spin	**2**	4	6	8	10
	Energy (A.U.)	**-1704.60**	-1704.57	-1704.48	-1704.38	-1704.28
	Energy difference (kJ mol^{-1})	**0**	+72	+327	+580	+802
Cu$_5$O$_5$C$_{12}$	Spin	2	**4**	6	8	10
	Energy (A.U.)	-1818.62	**-1818.62**	-1818.56	-1818.46	-1818.38
	Energy difference (kJ mol^{-1})	+2	**0**	+150	+405	+621
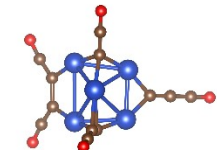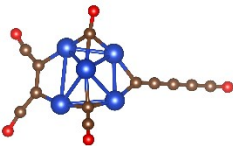
Table S7. Energies for the structures Pb$_4$O$_{4\text{-}6}$C$_{12}$ and Cu$_5$O$_5$C$_{12}$ found within 250 kJ mol^{-1} of the lowest energy structure. Energies shown for the singlet/triplet spin state for lead-based systems and doublet/quartet for copper-based. The most stable spin is highlighted in bold, and the energy difference given in brackets.
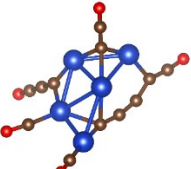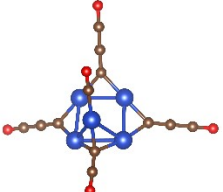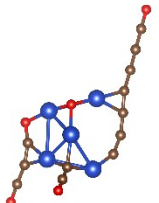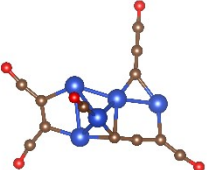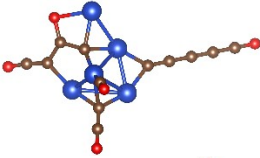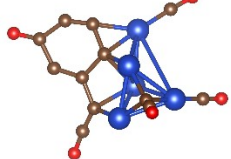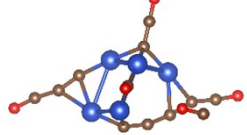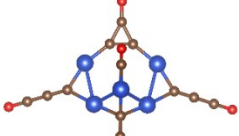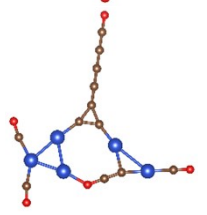
System	Structure	Energy (A.U.)		Energy difference from structure 1 (kJ mol^{-1})	
		Spin 1	Spin 3		
Pb$_4$O$_4$C$_{12}$	1	**-770.91**	-770.88 (+82 kJ mol)	0	
	2	-770.88 (+6 kJ mol^{-1})	**-770.88**	+82	
	3	**-770.87**	-770.84 (+78 kJ mol^{-1})	+121	
	4	**-770.86**	-770.80 (+154 kJ mol^{-1})	+142	
	5	**-770.85**	-770.84 (+32 kJ mol^{-1})	+172	
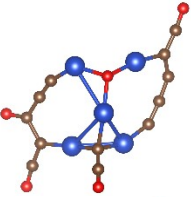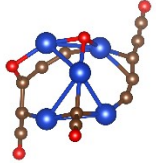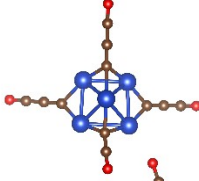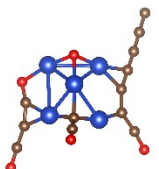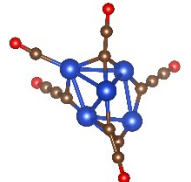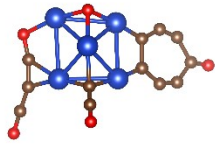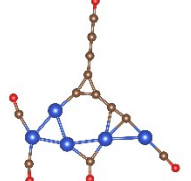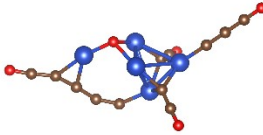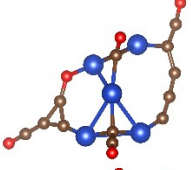
	6	**-770.84**	-770.81 (+87 kJ mol^{-1})	+195
	7	**-770.84**	-770.83 (+25 kJ mol^{-1})	+199
	8	**-770.84**	-770.83 (+15 kJ mol^{-1})	+204
	9	**-770.83**	-770.81 (+65 kJ mol^{-1})	+218
	10	**-770.83**	-770.78 (+117 kJ mol^{-1})	+230
	11	**-770.83**	-770.82 (+21 kJ mol^{-1})	+233
$Pb_4O_5C_{12}$	1	-846.09 (+48 kJ mol^{-1})	**-846.11**	0
	2	**-846.09**	-846.09 (+6 kJ mol^{-1})	+51
	3	-846.00 (+151 kJ mol^{-1})	**-846.06**	+130
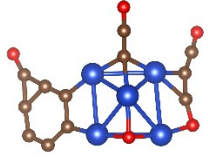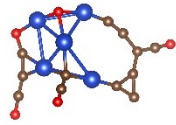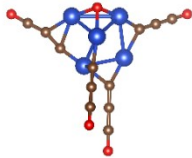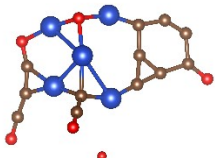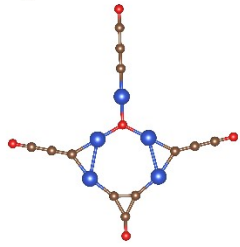
	4	-846.03 (+20 kJ mol^{-1})	**-846.04**	+180	
	5	**-846.04**	-846.02 (+35 kJ mol^{-1})	+182	
	6	**-846.03**	-846.01 (+46 kJ mol^{-1})	+214	
	7	**-846.02**	-846.00 (+57 kJ mol^{-1})	+216	
	8	**-846.02**	-846.00 (+51 kJ mol^{-1})	+218	
	9	-845.99 (+72 kJ mol^{-1})	**-846.02**	+236	
$Pb_4O_6C_{12}$	1	**-921.33**	-921.26 (+193 kJ mol^{-1})	0	
	2	**-921.33**	-921.31 (+39 kJ mol^{-1})	+7	
	3	-921.29 (+59 kJ mol^{-1})	**-921.31**	+43	

Structure	Spin 2	Spin 4	Energy difference	
4	**-921.28**	-921.27 (+36 kJ mol⁻¹)	+119	
5	**-921.27**	-921.24 (+86 kJ mol⁻¹)	+158	
6	**-921.25**	-921.21 (+102 kJ mol⁻¹)	+208	
7	**-921.24**	-921.22 (+53 kJ mol⁻¹)	+231	
8	**-921.24**	-921.22 (+39 kJ mol⁻¹)	+236	
9	**-921.23**	-921.22 (+51 kJ mol⁻¹)	+247	

System	Structure	Energy (A.U.)		Energy difference from structure 1 (kJ mol⁻¹)	
		Spin 2	Spin 4		
$Cu_5O_5C_{12}$	1	-1818.62 (+2 kJ mol⁻¹)	**-1818.62**	0	
	2	**-1818.62**	-1818.62 (+4 kJ mol⁻¹)	+2	

3	-1818.60 (+38 kJ mol^{-1})	**-1818.62**	+5
4	**-1818.61**	-1818.60 (+4 kJ mol^{-1})	+30
5	**-1818.61**	-1818.58 (+56 kJ mol^{-1})	+33
6	**-1818.60**	-1818.59 (+16 kJ mol^{-1})	+47
7	**-1818.60**	-1818.59 (+33 kJ mol^{-1})	+50
8	**-1818.59**	-1818.58 (+33 kJ mol^{-1})	+75
9	**-1818.57**	-1818.57 (+1 kJ mol^{-1})	+119
10	-1818.54 (+94 kJ mol^{-1})	**-1818.57**	+120
11	**-1818.57**	-1818.55 (+45 kJ mol^{-1})	+122

12	-1818.55 (+37 kJ mol^{-1})	**-1818.57**	+130
13	**-1818.57**	-1818.55 (+44 kJ mol^{-1})	+133
14	-1818.55 (+34 kJ mol^{-1})	**-1818.57**	+136
15	**-1818.56**	-1818.54 (+67 kJ mol^{-1})	+149
16	**-1818.56**	-1818.55 (+29 kJ mol^{-1})	+157
17	**-1818.56**	-1818.53 (+70 kJ mol^{-1})	+162
18	**-1818.55**	-1818.53 (+66 kJ mol^{-1})	+174
19	**-1818.55**	-1818.54 (+31 kJ mol^{-1})	+184
20	-1818.55 (+1 kJ mol^{-1})	**-1818.55**	+187
21	-1818.54 (+12 kJ mol^{-1})	-1818.55	+190

22	**-1818.54**	-1818.52 (+63 kJ mol^{-1})	+207	
23	**-1818.54**	-1818.52 (+50 kJ mol^{-1})	+208	
24	-1818.54 (+7 kJ mol^{-1})	**-1818.54**	+209	
25	**-1818.52**	-1818.5 (+63 kJ mol^{-1})	+245	
26	-1818.51 (+49 kJ mol^{-1})	**-1818.52**	+247	

References

1 J. S. Ogden and M. J. Ricks, *J. Chem. Phys*, 1972, **56**, 1658.

2 A. Popovič, A. Lesar, M. Guček and L. Bencze, *Rapid Commun. Mass Spectrom.*, 1997, **11**, 459–468.

3 G. V Chertihin and L. Andrews, *J. Chem. Phys*, 1996, **105**, 2561.

4 J. Drowart, R. Colin and G. Exsteen, *Trans. Faraday Soc.*, 1965, **61**, 1376–1383.

5 I. L. Christopher, A. A. L. Michalchuk, C. R. Pulham and C. A. Morrison, *Front. Chem.*, 2021, **9**, 1–13.